JOURNAL OF GEOPHYSICAL RESEARCH, VOL. 102, NO. D12, PAGES 13,473–13,486, JUNE 27, 1997

Estimation of the cyclostationary dependence in geophysical data fields

M. J. OrtizBeviá
Departamento de Física, Universidad de Alcalá, Madrid, Spain

Abstract. Geophysical multivariate data fields are frequently analyzed using linear inverse modelling. A cyclostationary dependence, whether annual, semiannual or diurnal, is usually present in these data. The dependence can be introduced in the inverse linear model in two different ways, known as the "fixed phase" and the "phase smoothed" approaches. When either of them is set to the analysis of real data, the interpretation of some of the diagnostics parameters is not straightforward. From statistical considerations, both methods are expected to perform rather loosely at some points. It is then hard to decide if those values of the parameters correspond to characteristics present in the observed field or to failures of the method. To settle this matter, we proceed in this work to analyze the same synthetic geophysical fields with both methods. The fields consist basically of geophysical waves of known frequency, upon which a cyclostationary dependence is imposed, that are embedded in noise. Different fields were generated by changing the phase of the cyclostationary dependence and the characteristics of the noise, and analyzed using both methods . Through this systematic procedure we assess the real meaning of the diagnostic parameters. Because the true signals and phase of the cyclostationary dependence are known, the performances of both approaches can be compared.

1. Introduction

Despite its simplicity and limitations, linear inverse modelling has proved to be very fruitful in the analysis of geophysical data (see, for instance, *Tarantola* [1987]). Many of the data fields analyzed present a dependence on a frequency that can be traced back to a cycle in the mean feedback (annual, semiannual or diurnal). This cyclostationary dependence is commonly removed by a filter, applied to the time series previous to the analysis. This is quite right if the analysis is focused in a range of frequencies that does not encompass the cyclic one. Nevertheless this procedure has several important drawbacks. The variability explained by the filtered field, for instance, is considerably smaller that the one present in the raw data. Additionally, the filtering can change the timing of some bigger fluctuations ("events") present in the data; this can be of importance if the parameters determined through the linear inverse modelling are intended as predictors.

On the other hand, the cyclostationarity can be taken into the linear inverse modelling. This can be done in two different ways, known as "fixed phase" and "phase smoothed". In the fixed phase approach, which is recommended in most classic statistical textbooks, the time series must be divided into subseries, each of them presenting the same phase, that is, the same stage of the cyclostationary dependence (i.e. if the cycle is the seasonal dependence and the observations are monthly, we will divide our time series in 12 subseries, one with all the Januaries, another with the Marches,..etc). Then the linear modelling can proceed on each subseries.

Paper number 97JD00243
0148-0227/97/97JD-00243$09.00

If m is the length of the original time series, and T_a is the number of observations in time required for one cycle (in the example above, 12), the partition of the series according to the value of the phase will leave us with T_a subseries of length (m/T_a). This points to the main problem of the phase fixed approach: to be feasible, m, the original time series length, must be considerably greater than T_a. Even if this is true, the error in the estimation of the parameters from these subseries will be always greater than if the parameters were estimated with all the length of the original series. If several signals with different cyclostationary dependence are present in the data, these errors in the estimation would possibly lead to a failure at separating them.

Another possible way of dealing with the cyclostationary dependence is to introduce the cyclic dependence into the parameters of the model, usually by expanding them into harmonics of the cyclic frequency. Because the expansion is truncated after a few terms, this procedure is known as the phase smoothed method. The big advantage of this method is that the parameters are estimated from the entire length of the time series. Thus, if the number of terms kept in the expansion is, for instance, three, we will need only three estimators to describe the cyclic evolution of each of the parameters of the model, while T_a estimators would be necessary when using the phase fixed method. Against this, the method presents an uncertainty concerning the phase of the cyclic evolution. That is, we would not know if the maximum value in the seasonal evolution of the large-scale pattern of variability corresponds to January or to April, for instance.

Both ways of modelling a cyclostationary dependence have been introduced into a linear autoregressive model for the evolution in time of the multivariate fields: the principal oscillation pattern (POP) analysis [*Hasselmann*, 1988]. Cy-

clostationary POP with the phase fixed approach have been used to analyze observed sea surface temperature (SST) in an equatorial band of the Indo-Pacific basin [*Storch et al.*, 1993]. The procedure applied in *Blumenthal* [1991] follows basically this approach, although with some phase-smoothed touch: the data are sampled every 3 months, and this can help to avoid some of the pitfalls of the fixed phase method. Cyclostationary POP with the phase smoothed approach were used to analyze winds and sea surface temperature (SST) data in the tropical band of the Indo-Pacific [*OrtizBeviá*, 1993]. All these works show how both approaches can be made operative to introduce the seasonality into the POP scheme. But on the basis of these applications, we cannot decide how well each method is performing. In the case of the ENSO (El Niño - The Southern Oscillation) simulated variability [*Blumenthal*,1991] we are limited by the simplicity of the model. And in the other cases, real data are too complex to give any clear answer. Then, as a consequence of these applications, we will end with new questions in addition to the old ones, as for instance the meaning of some values of the diagnostic parameters.

To answer them, several simulations of geophysical fields were analyzed with both techniques. The procedure followed to build the synthetic fields is described in section 3 of this paper. In section 2, after a brief account of the linear model used (the POP), we describe both methods of introducing seasonality into the linear inverese modeling. The output yielded by each approach is analyzed and compared in section 4. Because we know the characteristics of the signals present in these fields, we can assess the performance of each method and the meaning of the diagnostic parameters becomes clear.

2. Introduction of the Seasonality Into the Linear Model

Let $(z_{ij},\ i = 1,\cdots,m;\ j = 1,\cdots,n)$ be a set of $m \times n$ observations of the value of one or several physical variables (for instance sea level pressure or sea surface temperature) in n different grid points, at m different instants of time. We will use here $i = 1,\ldots,m$ to denote the time variability while $j = 1,\cdots,n$ will index the spatial dependence. For each instant of time j, the z_{ij} values for $j = 1,\ldots,n$, can be viewed as one realization of the state vector $\vec{z}$ (an array of one column and p rows). $\vec{z}^T$ will denote the transposed of a vector. In a statistical description, the data field could be characterized by its mean value vector $\bar{\vec{z}}$ and its covariance matrix $\mathbf{\Sigma}$, whose elements are respectively given by

$$\bar{\vec{z}} = \frac{1}{m}\sum_{i=1}^{m}\vec{z}_i \tag{1}$$

$$\mathbf{\Sigma} = \sum_{i=1}^{m}\frac{(\vec{z}_i - \bar{\vec{z}})(\vec{z}_i - \bar{\vec{z}})^T}{m}. \tag{2}$$

If the complexity of the system is great, as usually happens with geophysical observations, a reduction of the number of degrees of freedom is customary. Such reduction can be obtained through expansion of the variables of the system (the data at each point of the grid) in terms of some functions, followed by truncation. Both, a basis for the expansion and a criterion for the truncation can be obtained directely from the statistics of the field. The basis are the eigenvectors $\vec{e}_k$ of the covariance matrix $\mathbf{\Sigma}$, also known as empirical orthogonal functions (EOF), and the criterion is the amount of variance explained by the corresponding (real) eigenvector. By keeping only $l \ll n$ terms in the expansion, we are left with a filtered field:

$$z'_{ij} = \sum_{k=1}^{l} r_{ik}e_{kj}. \tag{3}$$

The time dependence in the original field is confined to the coefficients r_{ik} in the expansion, known as principal components (PC) of the field. When Fourier analyzed, they usually contain several (low) frequencies. The statistical technique known as POP analysis aims at separating these frequencies through the determination of a new spatial basis. To do this in the simplest way, we assume that the system evolution can be represented by an autoregressive first-order process (AR(1)). That is, the $\vec{r}_i$ coefficients satisfy the finite difference equation

$$\vec{r}_{i+1} - \vec{r}_i = \Delta t(\mathbf{A}\vec{r}_i + \vec{n}_i) \tag{4}$$

where $\mathbf{A}$ is the dynamical matrix of the AR(1) process. The above expression can alternatively be written as

$$\vec{r}_{i+1} = \mathbf{B}\vec{r}_i + \vec{n}_i \tag{5}$$

using the forward matrix $\mathbf{B} = (\mathbf{I} + \Delta t\mathbf{A})$ where $\mathbf{I}$ is the identity matrix. The stochastic characteristics of the field are taken care of by the term $\vec{n}_i$, representing a white noise. Matrix $\mathbf{B}$ can be estimated from the data through an LSE minimization procedure. The standard way in the POP literature is based in second moment statistics and yields $\mathbf{B} = \mathbf{C}_1\mathbf{C}_0^{-1}$ where $\mathbf{C}_1$ and $\mathbf{C}_0$ are the data covariance matrices at lags 1 and 0 respectively.

Solution of the deterministic part of (4) can be expressed as

$$\vec{r}_i = \sum_{k=1}^{l} c_k e^{\mu_k \Delta t_i}\vec{u}_k, \Delta t_i = t_i - t_0,\ i = 1,\cdots,m; \tag{6}$$

where the characteristic exponents μ_k can be obtained from the λ_k eigenvalues of the matrix $\mathbf{B}$: $\mu_k = \ln(\lambda_k)$, and where $\vec{u}_k$ are the corresponding eigenvectors. Because $\mathbf{B}$ is non-symmetric, both eigenvalues and eigenvectors will in general be complex. Also, due to the assumption of stationarity, $\mathrm{abs}(\lambda_k)$ must be smaller than 1, that is, μ_k is negative and the oscillation is always damped. If the number of complex eigenvalues is l_i, (6) can now be written as:

$$\vec{r}_i = \sum_{k=1}^{l_i} c_k e^{\mu_k \Delta t_i}(Re(\vec{u}_k) + \imath Im(\vec{u}_k)) + \sum_{k=l_i+1}^{l} c_k e^{\mu_k \Delta t_i}\vec{u}_k. \tag{7}$$

If we denote $\gamma_k \equiv Re(\mu_k)$ and $\omega_k \equiv Im(\mu_k)$, it is easy to work out that for each pair of complex conjugated eigenvalues, μ_k and μ_{k+1}, and we will have a pair of real patterns $\vec{p}_k = Re(\vec{u}_k)$ and $\vec{q}_k = Im(\vec{u}_k)$, associated to a frequency ω_k, a period T_k and a damping factor γ_k. These are the POP of the system at that frequency. For each POP, (7) prescribes the following evolution in time

$$\vec{p}_k \xrightarrow{T_k/4} -\vec{q}_k \xrightarrow{T_k/4} -\vec{p}_k \xrightarrow{T_k/4} \vec{q}_k. \tag{8}$$

The evolution in time for each pair can also be obtained empirically from the principal components. If we build a matrix $\mathbf{W}$ with elements $(\vec{w}_j = \vec{p}_j,\ \vec{w}_{j+1} = \vec{q}_j,\ j = 2k - 1,\ k = 1, l_i)$ and $\vec{w}_j = Re(\vec{u}_k),\ k = l_{i+1}, l$, then $\vec{r}_i = \mathbf{W}\vec{s}_i$ and the empirical time coefficients are given by

$$\vec{s}_i = \mathbf{W}^{-1}\vec{r}_i. \tag{9}$$

Comparison between the theoretical evolution of the pair of POP, given by (8), and that estimated by (9), will provide a measure of the suitability of the POP scheme for describing the evolution in time of the field $\{z_{i,j}\}$. The damping exponents, $-\gamma_k$, are other indicators of the "quality" of a pair of POP. After some time δT the most probable patterns to be observed are those corresponding to the POP with smaller damping exponents.

If we know that the physical system that produces the data field $\{z_{i,j}\}$ is under a cyclostationary feedback of period T_a, it is reasonable to asume that the data also will have a dependence on the same period, that is, $z_{i+T_a,j}$ will be related in a nonstochastic way to $z_{i,j}$. This dependence in time will go over into the $\vec{r}_i$, PC of the field, and therefore the dynamical matrix that describes the evolution of these coefficients will be periodic of period T_a:

$$\mathbf{A}_{(k+T_a)} = \mathbf{A}_k. \tag{10}$$

In the POP fixed phase approach the cyclostationarity is made explicit by writing $i = (iy-1)T_a + \kappa$, where iy indexes the order of the cycles T_a contained in i, and rewriting (4) as

$$\vec{r}^{\kappa}_{(iy+1)} - \vec{r}^{\kappa}_{iy} = \Delta t(\mathbf{A}^{\kappa}\vec{r}^{\kappa}_{iy} + \vec{n}_{iy}) \tag{11}$$

where κ denotes the phase of the cycle and $\Delta t = T_a$. Because the most common cyclostationary dependence in geophysical fields is the annual one, we will refer always to this case as an example. In our example κ will index the season of the year if the data are seasonal or will be the monthly index if they are monthly data. The system described by (4) is statistically nonstationary, but a stationary statistics can be recovered by fixing the value of κ. If this value is set to, for instance, κ_1, and for values of $\vec{r}$ that lie at lag T_a, the b_{jk} coefficients of (5) will not be dependent on time, and we will have an AR(1) relationship. Consequently, instead of only one, as in the stationary case, we will have T_a forward matrices $\mathbf{B}^{\kappa} = (\mathbf{I} + \Delta t\mathbf{A}^{\kappa})$. In our seasonal example that means that we will have a forward matrix $\mathbf{B}^1$ that will characterize the transition from one January to the next, another matrix $\mathbf{B}^2$ for the transition between Aprils, etc. The eigenvectors of each of these matrices will satisfy the relationship

$$\mathbf{B}^{\kappa}\vec{u}^{\kappa}_k = \lambda^{\kappa}_k\vec{u}^{\kappa}_k. \tag{12}$$

This set of T_a different eigenvalues and eigenvectors indexed by κ can be introduced to give an equivalent of (7)

$$\begin{aligned}\vec{r}_i &= \sum_{k=1}^{l_i} c^{\kappa}_k e^{(\gamma^{\kappa}_k + \imath\omega^{\kappa}_k)\Delta t_i}(Re(\vec{u}^{\kappa}_k) + \imath Im(\vec{u}^{\kappa}_k)) \\ &+ \sum_{k=l_i+1}^{l} c^{\kappa}_k e^{\mu^{\kappa}_k \Delta t_i}\vec{u}^{\kappa}_k \end{aligned} \tag{13}$$

but the POP evolution scheme given by (8) will hold only if we can write $\omega^{\kappa}_k \equiv \omega_k$. *Blumenthal* [1991] gives a proof of such identity. Then for each frequency ω_k there will be T_a pairs of real seasonal patterns $\vec{p}^{\kappa}_k = Re(\vec{u}^{\kappa}_k)$ and $\vec{q}^{\kappa}_k = Im(\vec{u}^{\kappa}_k)$, which will give the cyclostationary evolution of the $\vec{p}_k$ and $\vec{q}_k$ associated to the ω_k frequency. If the $\vec{p}_k$ is observed at season κ_1, the evolution in time prescribed by the POP evolution scheme will establish

$$\vec{p}_k^{\,\kappa_1} \xrightarrow{T_k/4} -\vec{q}_k^{\,\kappa_2} \xrightarrow{T_k/4} -\vec{p}_k^{\,\kappa_3} \xrightarrow{T_k/4} \vec{q}_k^{\,\kappa_4} \tag{14}$$

where $\kappa_i + T_k/4 = \kappa_j + nT_a$.

Blumenthal's [1991] proof requires the definition of seasonal transition matrix between phase stages κ and $\kappa+1$, $\mathbf{M}^{\kappa}$,

$$\vec{r}^{\kappa+1} = \mathbf{M}^{\kappa}\vec{r}^{\kappa} + \vec{n}. \tag{15}$$

The cyclostationarity implies $iy + n\kappa \equiv (iy+1) + \kappa$ and $\mathbf{M}^{\kappa+n} \equiv \mathbf{M}^{\kappa}$. It is then easy to show that matrix $\mathbf{B}^{\kappa}$, which forwards the state of the system at one season to the same season the following year, can be written as a product of the seasonal transition matrices,

$$\mathbf{B}^{\kappa} = \mathbf{M}^{(\kappa+n-1)}\mathbf{M}^{(\kappa+n-2)}\cdots\mathbf{M}^{\kappa}. \tag{16}$$

If transition matrix $\mathbf{M}^{(\kappa+n)}$ is then applied to both sides of the eigenvalue equation (12)

$$\mathbf{M}^{(\kappa+n)}\mathbf{B}^{\kappa}\vec{u}^{\kappa}_k = \mathbf{B}^{(\kappa+1)}\mathbf{M}^{\kappa}\vec{u}^{\kappa}_k = \lambda^{\kappa}_k\mathbf{M}^{(\kappa+n)}\vec{u}^{\kappa}_k \tag{17}$$

which proves that the eigenvalues of matrix $\mathbf{B}^{(\kappa+1)}$ and its eigenvectors can be obtained as

$$\lambda^{(\kappa+1)}_k = \lambda^{\kappa}_k \tag{18}$$

$$\vec{u}^{(\kappa+1)}_k = \mathbf{M}^{\kappa}\vec{u}^{\kappa}_k. \tag{19}$$

Because all the $\mathbf{B}^{\kappa}$ share the same eigenvalues, the phase dependence of the POP must be inferred either from the eigenectors $\vec{u}^{\kappa}_k$ [*Storch et al*, 1993] or from the eigenvalues of the transition matrices $\mathbf{M}^{\kappa}$ [*Blumenthal*, 1991].

If κ is chosen as the initial state season, the normalization constant $n^{(\kappa+1)}_k$

$$n^{(\kappa+1)}_k = \| \mathbf{M}^{\kappa}\vec{u}^{\kappa}_k \| \tag{20}$$

can spot the stage of the cycle of a season $(\kappa+1)$ referred to the κ season.

Introducing the seasonality into our model yields a more realistic evolution scheme. We hope that this relatively minor complexity (the model is always linear), will allows us to make better predictions. There is in particular one case when the cyclostationary POP gives a meaningful description of the evolution of a system: when T_k the period associated to the k pair of POP contains an exact number of times the cyclostationary period T_a. For instance, if $\omega_k = 0.5\omega_a$ and we start by observing the pattern $\vec{p}_k$ at season 1, pattern $-\vec{q}_k$ will be observed at season 3, pattern $-\vec{p}_k$ will appear again at season 1, and pattern $\vec{q}_k$ at season 3. We will say that this pair of POP is locked to the seasonal cycle, and we will expect the values of the damping factor to reflect this fact.

In the POP phase smoothed method the cyclostationary dependence of matrix $\mathbf{A}$ could be modelled as

$$\mathbf{A}(t) = \mathbf{A}_0 + \mathbf{A}_1\cos(\omega_a t) + \mathbf{A}_2\sin(\omega_a t) \tag{21}$$

$\omega_a = 2\pi/T_a$ being the frequency of the cyclic feedback, that it is assumed to be known "a priori". As in the stationary case, B_{jk} has to be determined from the data using a LSE fit between the time series and the modelled matrix.

The theory of linear systems of Floquet (see the appendix) allow us to represent the solution to (4) as

$$\vec{r}_i = \sum_{k=1}^{l} c_k e^{\mu_k \Delta t_i}\vec{u}_k, \Delta t_i = t_i - t_0,\ i = 1,\cdots,m; \tag{22}$$

where the μ_k are no longer obtained from the λ_k, the eigenvalues of the forward matrix $\mathbf{B}$, but from those of a char-

acteristic matrix Ψ. Similarly, the $\vec{u}_k$,no longer constant in time but periodic with period T_a, can be obtained from a fundamental matrix $\mathbf{Y}$

$$\vec{u}_k = Y_i(t_l)e^{-\mu_k \Delta t_l}, \Delta t_l = t_l - t_0 \; l = 1, 2, \cdots, T_a. \quad (23)$$

As in the stationary case, λ_k ,the eigenvalues of the characteristic matrix will in general be complex. For each pair of complex conjugated eigenvalues, λ_k and λ_{k+1}, we will have a pair of real patterns $\vec{p}_k = Re(\vec{u}_k)$ and $\vec{q}_k = Im(\vec{u}_k)$, associated to a frequency ω_k and a period T_k. These will be the POP of the system at that frequency and will satisfy (14). The stationary part of these patterns can be separated by averaging to the seasonal cycle.

$$p_{ks} = \frac{1}{T_a}\sum_{i=1}^{T_a} p_{ik}. \quad (24)$$

For some seasons the stationary pattern will be reinforced, while for others it will be weakened. During these last seasons, transition from pattern 1 to pattern -2 will take place preferentially. The POP evolution scheme will persist, but the steadiness of the evolution will be affected by the seasonal modulation in the strentgh of the pattern. The procedure followed in the phase smoothed analyses is summarized in Figure 1.

3. Determination of the Parameters of the Linear Cyclostationary Model

The dynamical matrices used in the POP phase fixed method are determined through an LSE fit. This can be done following the Yule-Walker procedure as in the stationary case: both members of (11) are multiplied by $\vec{r}_{iy}^{\kappa\,T}$ and averaged to the length of the time series. For each κ we will obtain an expression of the form

$$\mathbf{C}_1^{\kappa} = (\mathbf{I} + T_a\mathbf{A}^{\kappa})\,\mathbf{C}_0^{\kappa} \quad (25)$$

where $\mathbf{C}_1^{\kappa} = \{< \vec{r}_{iy+1}^{\kappa}\vec{r}_{iy}^{\kappa\,T} >\}$ and $\mathbf{C}_0^{\kappa} = \{< \vec{r}_{iy}^{\kappa}\vec{r}_{iy}^{\kappa\,T} >\}$, where (<>) indicates averaging to the time, and from which the values of $\mathbf{B}^{\kappa}$ can be derived.

Similarly, the three matrices used in the POP phase smoothed method can be determined from the three equations obtained by multiplying the expresion (4), with $\mathbf{A}$ given by (II.21), by $(\vec{r}_i^{\,T})$, by $(\cos(\omega_a i)\vec{r}_i^{\,T})$ and by $(\sin(\omega_a i)\vec{r}_i^{\,T})$. By averaging to the time (<>), one obtains a system of three linear equations

$$\mathbf{C}_1 = (\mathbf{I} + (\Delta t)\mathbf{A}_0)\,\mathbf{C}_0 + (\Delta t)\mathbf{A}_1\mathbf{C}_{0c} + (\Delta t)\mathbf{A}_2\mathbf{C}_{0s} \quad (26)$$

$$\mathbf{C}_{1c} = (\mathbf{I} + (\Delta t)\mathbf{A}_0)\,\mathbf{C}_{0c} + (\Delta t)\mathbf{A}_1\mathbf{D}_{0c} + (\Delta t)\mathbf{A}_2\mathbf{D}_{0cs} \quad (27)$$

$$\mathbf{C}_{1s} = (\mathbf{I} + (\Delta t)\mathbf{A}_0)\,\mathbf{C}_{0s} + (\Delta t)\mathbf{A}_1\mathbf{D}_{0cs} + (\Delta t)\mathbf{A}_2\mathbf{D}_{0s} \quad (28)$$

where

$$\begin{aligned}
\Delta t &= 1 \\
\mathbf{C}_1 &= \{< \vec{r}_{i+1}\vec{r}_i^{\,T} >\} \\
\mathbf{C}_0 &= \{< \vec{r}_i\vec{r}_i^{\,T} >\} \\
\mathbf{C}_{1c} &= \{< \vec{r}_{i+1}\cos(\omega_a i)\vec{r}_i^{\,T} >\} \\
\mathbf{C}_{1s} &= \{< \vec{r}_{i+1}\sin(\omega_a i)\vec{r}_i^{\,T} >\} \\
\mathbf{C}_{0c} &= \{< \vec{r}_i\cos(\omega_a i)\vec{r}_i^{\,T} >\} \\
\mathbf{C}_{0s} &= \{< \vec{r}_i\sin(\omega_a i)\vec{r}_i^{\,T} >\} \\
\mathbf{D}_{0c} &= \{< \vec{r}_i(\cos(\omega_a i))^2\vec{r}_i^{\,T} >\} \\
\mathbf{D}_{0s} &= \{< \vec{r}_i(\sin(\omega_a i))^2\vec{r}_i^{\,T} >\} \\
\mathbf{D}_{0cs} &= \{< \vec{r}_i\cos(\omega_a i)\sin(\omega_a i)\vec{r}_i^{\,T} >\}.
\end{aligned}$$

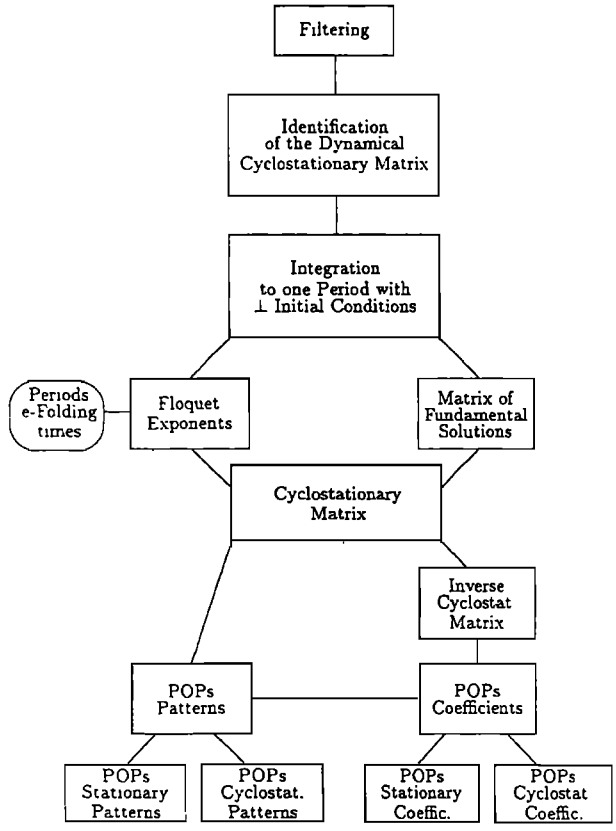

Figure 1. Flow diagram of the Cyclostationary POP procedure

From the above equations, the values of $\mathbf{A}_0$, $\mathbf{A}_1$, and $\mathbf{A}_2$ can be derived.

To determine $\mathbf{A}_0$, $\mathbf{A}_1$ and $\mathbf{A}_2$ one can also use standard leastsquares routines from NAG, IMSL or NR. Results using this last procedure do not differ much of the ones obtained with the Yule-Walker method.

4. Description of the Synthetic Data Fields

In the preceding section, we have seen that both methods rely on some 'ad hoc' assumptions. In this section we proceed to use both of them to analyze the same synthetic datasets. The points we were most interested in testing were the following: (1) The ability to identify the same POP at different seasonal stages (that is, test if $\omega_k^{\kappa_i} \equiv \omega_k^{\kappa_j}$). This can be better assessed if more than one signal is present in the data.(2) The ability to identify the phase of the seasonal dependence (that is, if the maximum of the variability took place in January or in May). Several fields with the same signals and different values of the phase had to be analyzed. (3) The accuracy in the determination of the waves characteristics (frequency, spatial patterns)

An obvious choice for the synthetic signals would have been a multivariate AR(1) proccess. It is relatively easy to generate an AR(1) field where several oscillations of different frequencies are present. But such features as the ratio between these frequencies, propagating or standing characteristics of the oscillation, and damping or locking to the seasonal cycle are hard to control in such processes. In our analysis it was most important to know beforehand these features, and therefore another procedure was followed

Table 1. Model Parameters, Typical Values and Description

Parameter	Typical value	Description
H	4 km	atmosphere height
c	200 ms^{-1}	horizontal velocity scale
$a = \sqrt{(c/2\beta)}$	2085 km	Rossby radius
$\tau = a/c$	1 hour	characteristic time scale
δt	1/4 hour	time step of the simulation
β	2.3 $\times 10^{-11}$ m^{-1} s^{-1}	variation of the Coriolis parameter f with latitude

to generate the fields. The synthetic fields were obtained by adding stochastic noise to some deterministic signals (waves).

The deterministic signals present in the different simulations are always the same. The atmospheric variability is represented by the fluctuations of the zonal velocity of a barotropic model. In such a model, the atmosphere is represented by a single layer of height H [*Matsuno*, 1966], in a band that goes from 40° S to 40° N. The Coriolis factor is assumed $f = \beta y$, where y is the latitudinal coordinate. Values of the parameters of this model are detailed in Table 1. The waves included in our model correspond to (1) an eastward gravity wave of $n = 1$, $k = 1$, and period $T_1 = 12$ hours and (2) an eastward propagating gravity wave, with $n = 0$, $k = 0.5$, and period $T_g = 20$ hours. The fluctuations of the zonal velocity u are obtained directly from the expresions

$$u = (\omega_{nl} - k)\psi_{n+1} + n(\omega_{nl} + k)\psi_{n-1} \tag{29}$$

where $\psi_n = e^{-(1/2)y^2} H_{n(y)}$ and $H_{n(y)}$ are the Hermite polynomials of order n and the frequency ω_n is the solution of the cubic equation

$$\omega_n^3 - k^2 + k\omega_n^{-1} = 2n + 1. \tag{30}$$

The selected wave frequencies are of the same order of magnitude but nevertheless well separated, and their spatial patterns, represented in Figure 3a (k=0.5) and in Figure 3b (k=1), are clearly distinct.

To impose the cyclostationary dependence on this field we look to the seasonal dependence of observed atmospheric fields. The plot in Figure 2 represents the power spectrum of an atmospheric field, the monthly observations of the zonal wind in the tropical band of the Pacific basin [*Barnett*, (1984)]. In this case the cycle is the real seasonal cycle. If one filters to get rid of the cyclostationary dependence, 23.5% of the field variance will be lost.

Many atmospheric fields power spectra will have the "red noise" look of Figure 2. There will be peaks at locations corresponding to the characteristic low frequencies in addition to more than one peak in the neigbourhood of the cycle's frequency ($\omega_a = 0.523$ $month^{-1}$ in Figure 2). To simulate this feature in our synthetic field, the cyclostationary dependence must modulate only part of the signal. Such a field (thereinafter referred to as the benchmark field) could be described by:

$$u_{ij} = (u^0_{ij} + u^1_{ij})\cos(w_a i + \theta_j) + (u^0_{ij} + u^1_{ij}) + n_{ij} \tag{31}$$

where u^0_{ij} is the value of the gravity wave of $n = 0$ and $k = 0.5$, and u^1_{ij} the value of the gravity wave of $n = 1$ and $k = 1$ at the j point of the grid and the i instant of time; n_{ij} represents the contribution of the noise to the value of the field at this point and instant of time. Notice that the noise is simply added to the deterministic signal (instead of contributing to the derivative of the field, as it should be in an AR(1) process). The cyclostationary dependence appears as a factor that modulates only a part of the signals; θ_j represents the phase of the cyclostationary dependence at each point j of the grid. In the present simulation $T_a = 4$ hours. The time step of the simulation was chosen for 1/4 of 1 hour, and the time series consist of $m = 432$ points or 27 feedback cycles. With this value of the cyclostationary dependence, the signal with a period of 12 hours will be locked to the cycle imposed.

The different simulations are obtained by changing the characteristics and the intensity of the stochastic noise added to the signal. We will use basically a white noise that consists of fluctuations that are uncorrelated in time and space and with an uniform distribution in the frequency domain. In some of the simulations, the noise added to the deterministic signal is red, obtained from the white one through a recursive three-point moving average. In all the cases analyzed the amount and characteristics of the noise are such that the signals cannot be identified visually (look,

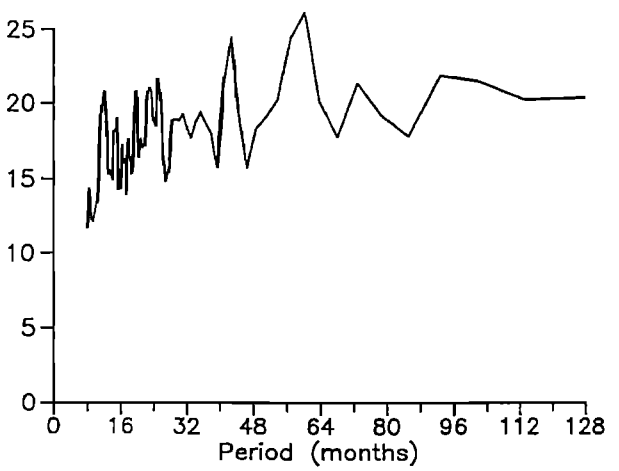

Figure 2. Example of observed atmospheric power spectrum. We show here the spatial average (to all grid points) of the power spectrum of zonal wind data in the Indopacific region [*Barnett*, 1984]

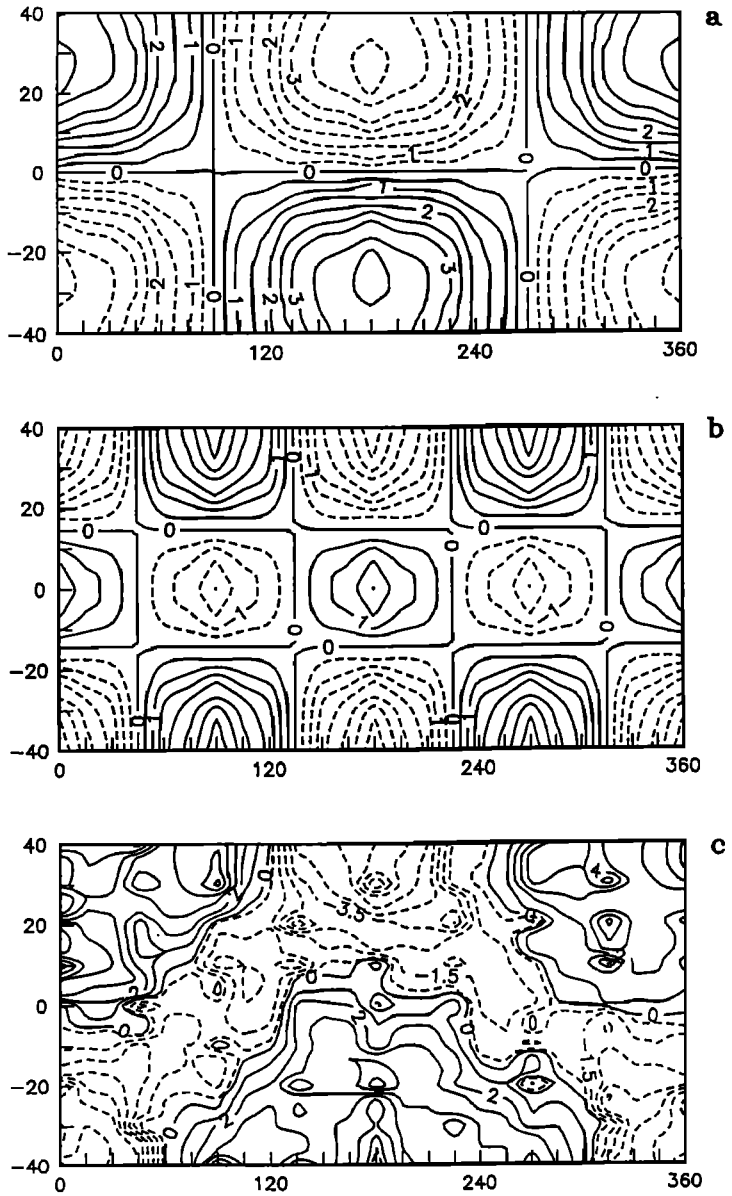

Figure 3. Longitude-latitude snapshot at $t = 1$ of the zonal velocity component of (a) the gravity wave with $n = 0, k = 0.5$, $T = 20$ hours; (b) the gravity wave with $n = 1$, $k = 1.$, $T = 12$ hours; and (c) the whole simplified field. The time step unit (t.u.) is 1/4 hour.

for instance, at Figure 3c where we show a snapshot of one of the fields analyzed).

The state of our atmosphere will be characterized by the values of u given by (31) and the noise n_{ij} is assumed to be white, of variance of $\sigma = 0.4$. Because we are used to thinking in terms of the seasonal cycle of 12 months, we will also refer to our 4-hour cycle in this way. Therefore the first hour in the cycle will be called season 1; the second, season 2; etc. Notice that because of the time step used for the sampling, in one cycle season 1 will be represented by the label 1, season 2 by the label 5, and so on. If, for instance, the value of the phase $\theta_j = 0$, because of the cyclostationary dependence imposed, we expect the signals in our field to be better observed in season 1 and season 2, because in seasons 3 and 4 our field will contain less signal.

Initially, the number of degrees of freedom of our field is the number of grid points, that is $n = 289$. After an expansion in the EOF of the field, only four terms were kept, which account for a 75% of the variance of the field. The time dependence will go into the $\vec{r}_k$, known as PC.

A simplified version of our benchmark field is obtained by dropping in (31) the term that is not seasonally dependent. The value of this simplified field would be given by:

$$u_{ij} = (u^0_{ij} + u^1_{ij})\cos(w_a i + \theta_j) + n_{ij}. \qquad (32)$$

Notice that in this case, if we assume for simplicity that the phase $\theta_j = 0$, the field for seasons 2 and 4 will contain almost no signal. In the next section, much attention will be paid to the analysis of this simplified field. Our benchmark field is quite simple but the interpretation of some values of its diagnostic parameters is not immediate. The interpretation of the ones obtained from the simplified field is always obvious. Therefore in the next sections the analyses of the simplified field will precede the ones of the benchmark field.

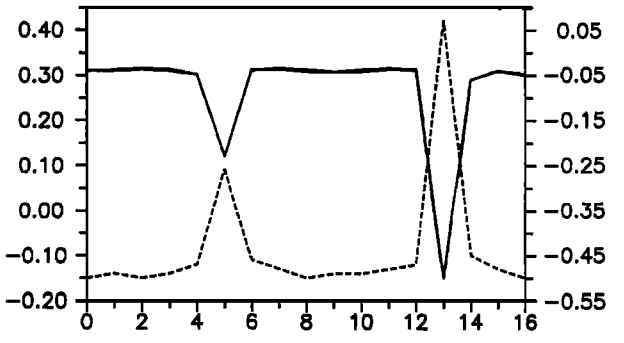

Figure 4. Simplified field with $\theta = 0$. Results of the fixed phase analysis. The figure shows the dependence of the real part of the characteristic exponent γ_1 (solid line) and γ_3 (dashed line) on the stages of the seasonal cycle. The length of the seasonal cycle is 4 hours, and the time step 1/4 hour. Notice how the jumps are located at the nodes (season 2 and 4) of the cyclostationary modulation. The straight lines represent the estimation of the same parameters by the phase smoothed method. Units for the solid lines are on the left, those for the dashed ones are on the right.

5. Intercomparison of the Cyclostationary Analyses

5.1. Ability to Identify the Same POP at Different Seasonal Stages

In first place, we applied the fixed phase method to the simplified field. The four time series of the first four PCs were separated into 16 subseries according to the 16 different stages of the cycle sampled. Each of them consists of 27 data maps. The 16 subseries were analyzed with the stationary POP model. From each of these subseries, a matrix $\mathbf{B}^\kappa$ was identified. The number of complex eigenvalues and therefore the number of pairs of POP obtained for each of the matrices varied from two to four. This was not inconvenient because for each matrix there was always one pair associated with the lower frequency (surprisingly, because the other is better sampled), and it was easy to establish a correspondence between the second pair of POP identified at some stages of the cycle and the two real POP appearing at other stages. For this analysis an interpretation is easily obtained from the real part of the characteristic exponent at each season, γ_k^κ. In Figure 4 we have represented the evolution of the γ_1^κ and γ_3^κ of our simplified field with κ, the stage of the cycle. The seasonal evolution of the first pattern of the pair 1/2 is plotted in Figure 5. Each seasonal pattern represented is the eigenvector corresponding to the first pair of complex eigenvalues of the matrices identified at the first, second, third and fourth hours of the cycle, which here are referred to as season 1, 2, 3, and 4, respectively.

Against expectations, there is a dependence of the real part of the γ_k^κ on κ, noticeable in Figure 4 as a jump at the first observation of season 2 and season 4. This means that although (16) is of course true, it does not hold when matrix $\mathbf{B}^\kappa$ in the left-hand side is estimated by (11) while in the right hand we have the transition matrices $\mathbf{M}^\kappa$ estimated using (16). When $\mathbf{B}^\kappa$ is estimated by (11), only the signal/noise ratio at the stage κ determines the errors; when estimated by the right-hand side of (16) the signal/noise ra-

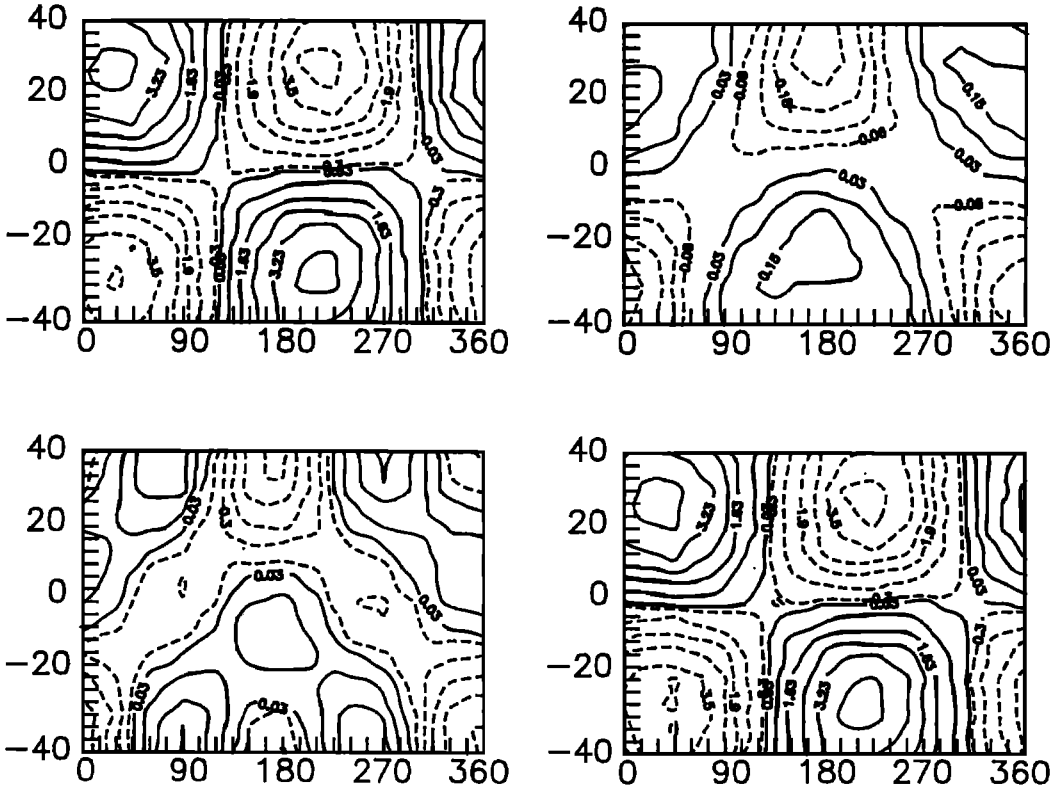

Figure 5. Simplified field. Results of the fixed phase analysis. Longitude-latitude representation of pattern 1 of the pair of POP 1/2. Beginning top left and clockwise, season 1, season 2, season 3, and season 4.

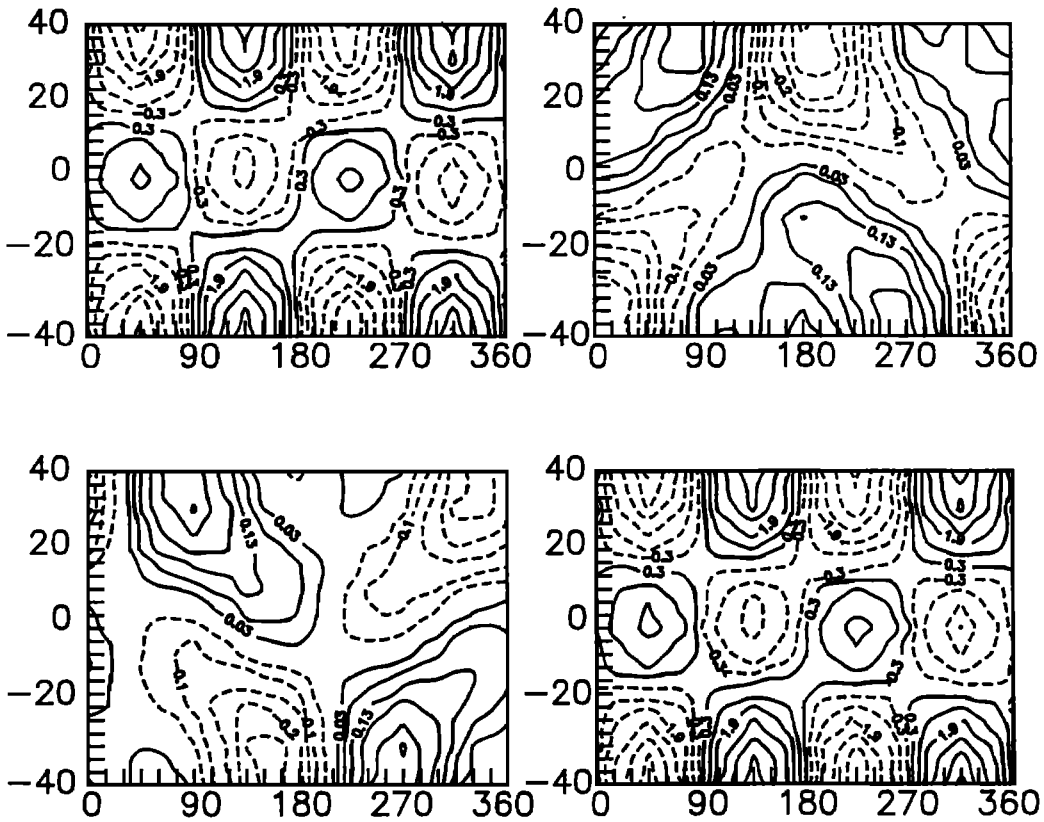

Figure 6. Simplified field. Results of the fixed phase analysis. Longitude-latitude representation of pattern 3 of the pair of POP 3/4. Beginning top left and clockwise, season 1, season 2, season 3, and season 4. Notice how the signals are not well separated in season 3, and compare with the results given by the phase smoothed method, represented in Figure 8.

tios of all stages present in one cycle are involved. In this way the γ_k^κ parameters, obtained from the eigenvalues of the forward matrices $\mathbf{B}^\kappa$ of the phase fixed method, allow for the identification of the stage of the cycle. This identification could be done also through the eigenvalues of the transition matrices $\mathbf{M}^\kappa$ as by *Blumenthal* [1991]. On the other hand, if we look at Figure 5, it is evident that this method fails at separating the signals. The spatial pattern represented corresponds to the wave with $n = 0$, of Figure 3a. Its "seasonal" evolution can be easily spotted at season 1 and 3, but at seasons 2 and 4 the pattern resembles more the spatial structure of the wave with $n = 1$, as represented in Figure 3b. In Figure 6 we have represented the seasonal evolution of the second pair of POP: we can see that at seasons 1 and 3, the pattern identified correspond to the wave with $n = 1$, of Figure 3b, while at seasons 2 and 4 the (noisy) pattern is rather similar to the one of the wave with $n = 0$. What happens here is not merely the replacement of one spatial pattern by the other, because the estimation of the frequencies is wrong also, as evidenced in Figure 7. The asymmetries in the "jumps" of Figure 4 can now be understood as a diagnostic of the intermixing of both POP at some seasons. This is a characteristic of the analysis with the fixed phase method confirmed in all our simulations.

Also in Figure 7 it can be seen how the phase smoothed analysis succeeds at separating the frequencies of the signals, as expected from theoretical considerations. Figure 8, where the seasonal evolution of the first POP of the pair 3/4 is represented, shows that this approach succeeds also at separating the spatial patterns (by contrast to Figures 5 and 6) The evolution of the pair 1/2 (not shown) represents well the other wave, with n=0. and k=.5. The similarity between Figure 9, where the stationary parts of the cyclostationary patterns identified are plotted, and Figures 3a and 3b, is quite satisfactory. But as the analyzed field (simplified case) has no stationary term, we must realize that the rate of the stationary/cyclostationary patterns can be

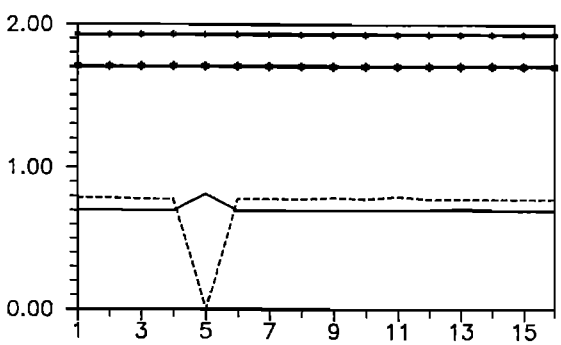

Figure 7. Simplified field. Estimation of the waves' frequencies given by both cyclostationary POP methods at different stages of the seasonal cycle. The straight lines with diamonds represent the estimation with the phase smoothed method. Below, solid and dashed lines give the estimation of the fixed phase procedure. The values used in the simulation were 1.28 for the POP 3/4 and 2.11 for the POP 1/2. The x axis extends to one cycle of the forcing (16 time steps).

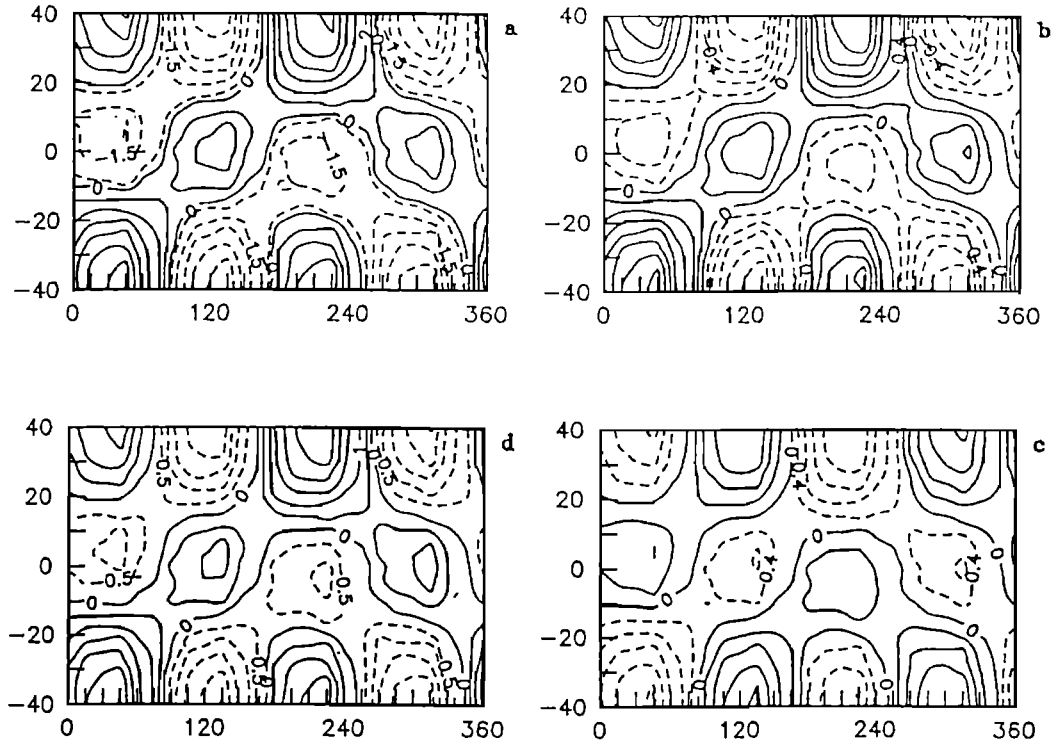

Figure 8. Simplified field. Results of the phase smoothed analysis. Longitude-latitude representation of pattern 3 of the pair of POP 3/4. Beginning top left and clockwise season 1, season 2, season 3, season 4.

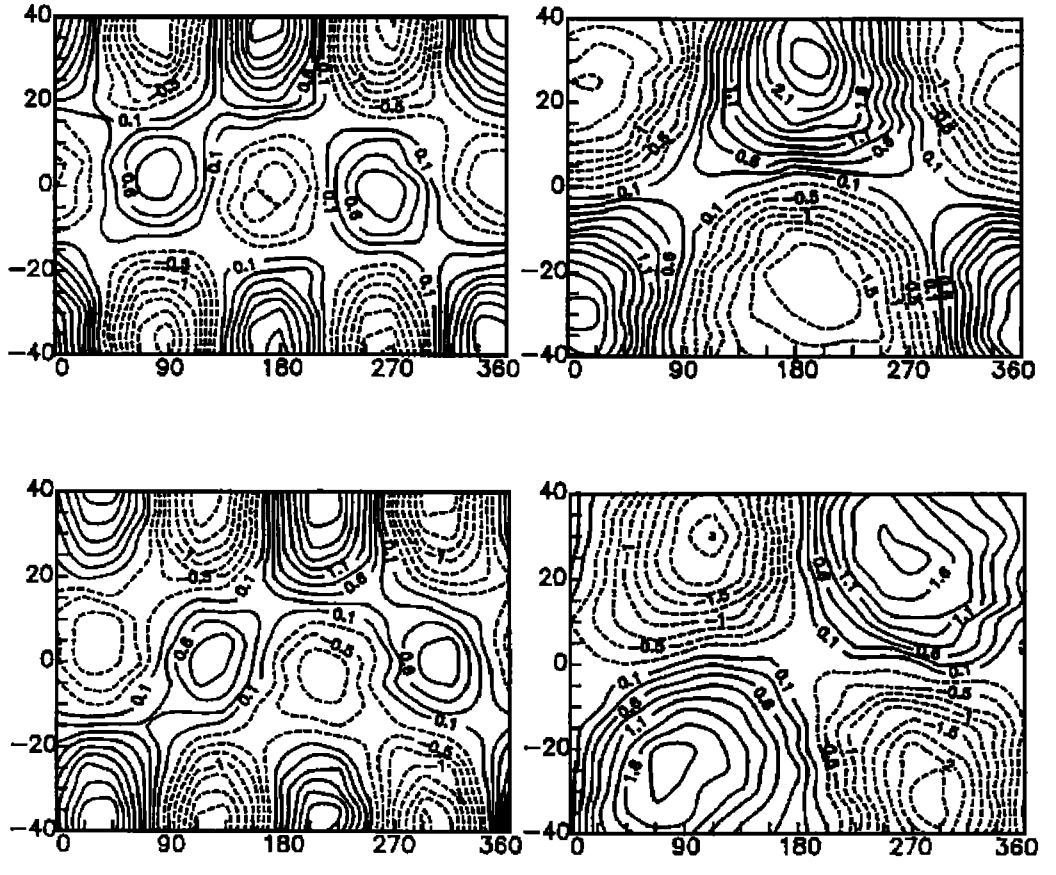

Figure 9. Simplified field. Results of the phase smoothed analysis. Longitude-latitude representation of the stationary part of the pair of POP 3/4 (left, top and bottom) and the pair of POP 1/2 (right).

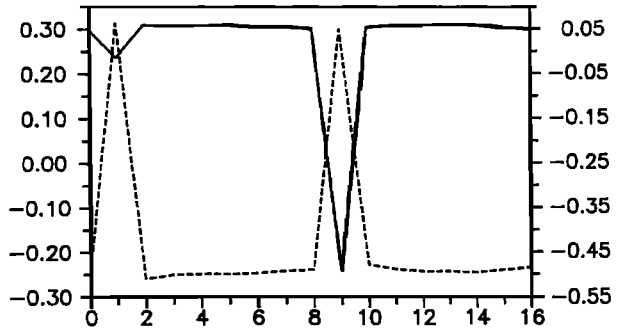

Figure 10. Simplified field with $\theta = \pi/2$. Results from the fixed phase analysis. Seasonal evolution of the real part of the exponent 1 of the first pair of POP (solid line) and 3 of the second pair (dashed line). Units as in Figure 4.

taken as a measure of the error in the determination of the Floquet exponents of our system. In all our simulations of the simplified field this relative error was roughly 10% of the cyclostationary pattern.

On the other hand, the phase smoothed method fails in the seasonal identification of the stages of the evolution plotted in Figure 8. This, evidenced by the experiments reported in the next section, could also be expected from theoretical considerations (the model proposed being a finite diference equation).

5.2. Ability to Identify the Phase of the Seasonal Dependence

To highlight this expected flaw of the phase smoothed procedure, a number of sensitivity experiments were performed. The fields analyzed correspond to the simplified case, given by (32); but for each simulation a different value of the phase θ was chosen. We will refer here to the case $\theta = \pi/2$, because all the other experiments support the conclusions obtained with this one. The evolution with the season of the real part of the characteristic exponents identified by the fixed phase method is represented in Figure 10. Although the asymmetries in the jumps are more noticeable in one of them, the change in the value of the phase could be identified easily.

In principle, the cyclic dependence of the pair of POP identified with the phase smoothed method is confined to the patterns. To estimate it, one can separate the cyclostationary POP vector $\vec{w}_i$ in a stationary $\vec{w}^s$ and a cyclostationary $\vec{w}_i^c$ term:

$$\vec{w}_i = \vec{w}_i^c + \vec{w}^s \tag{33}$$

and afterwards define the normalized projections

$$\vec{c}_i = \frac{\vec{w}_i^c \cdot \vec{w}^s}{\| \vec{w}_i^c \| \| \vec{w}^s \|}. \tag{34}$$

But in fact, this parameter shows very little variation when analyzing fields with different phase dependences (going from 0 to $\pi/2$).

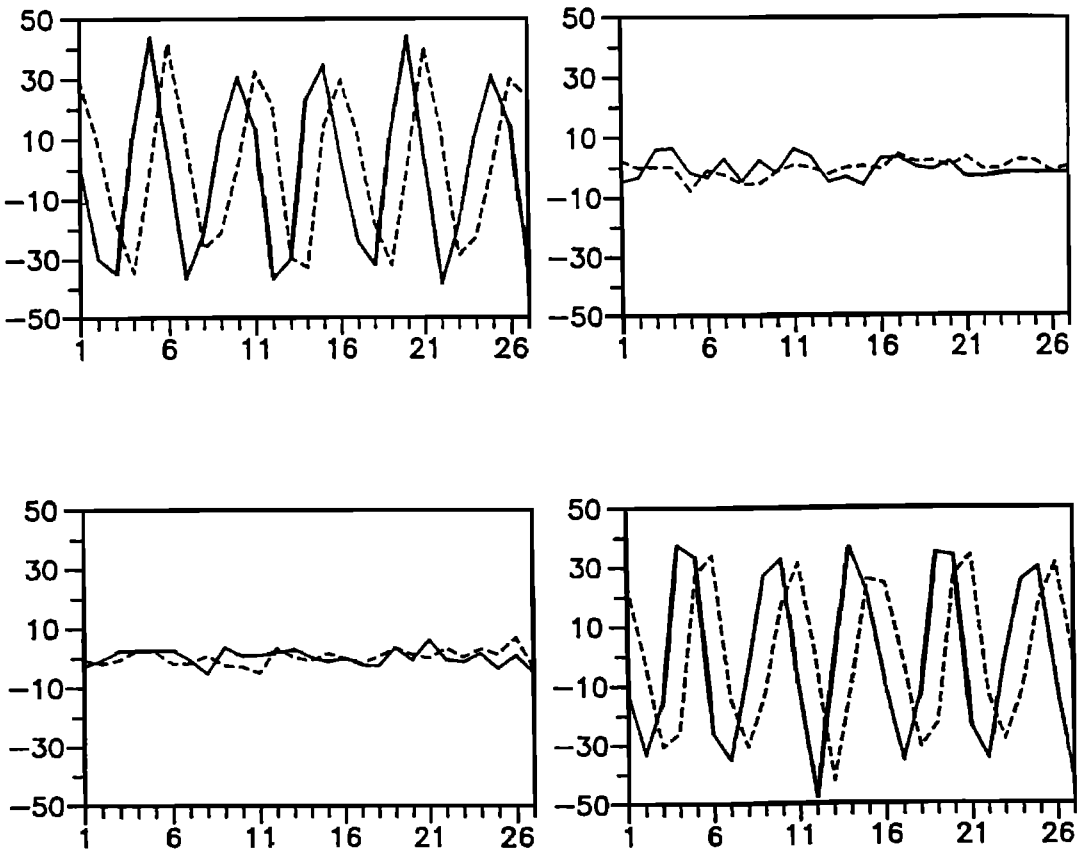

Figure 11. Simplified field with $\theta = 0$. Results of the phase smoothed analysis. Begining top left and clockwise, time coefficients of patterns 1 (solid) and 2 (dashed) of the pair 1/2, sorted by the season. The unit in the x axis is one seasonal cycle (in our case 4 hours) , the unit on the y axis is arbitrary.

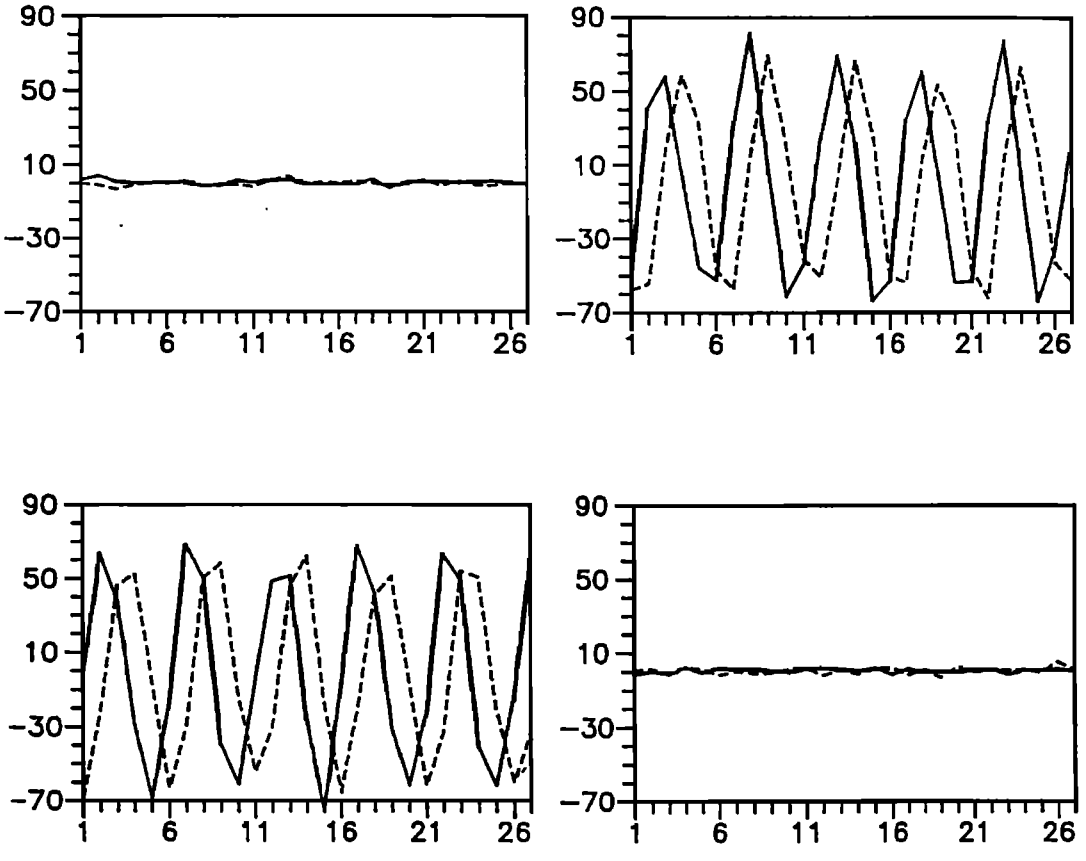

Figure 12. As in Figure 11 but for $\theta = \pi/2$.

Fortunately, the value of the phase of the seasonal dependence at each time step can be recovered from another parameter: the empirical time coefficients of the cyclostationary part of the POP patterns. The time coefficients obtained as in (9) can be split using the procedure of (33):

$$\vec{s}_i = \vec{s}_i^c + \vec{s}_i^s = \sum_k r_{ik}\vec{w}_k'^c + \sum_k r_{ik}\vec{w}_k'^s. \qquad (35)$$

For the case $\theta = 0$ and for the pair 1/2 the time coefficients $\vec{s}_i^c$, sorted according to the season, are represented in Figure 11. Figure 12 represents the same coefficients at the same seasons but for the case $\theta = \pi/2$. Notice how the phase of the cyclostationary dependence is sucessfully spotted by these time coefficients. At the months where there is a node in the deterministic field, the coefficients show only noise, while the signal appears clearly at the other extremals.

The results of the analysis of our benchmark field with the phase fixed method are shown in Figure 13. The real part of the eigenvalue for each pair of patterns identifies the summer as the unstable season. To explain this apparent paradox (the phase of the analyzed field is $\theta = 0$), we must realize that the deterministic signal in our benchmark field is never brought to zero by the cyclostationary dependence, because of the second term in the right-hand side of (31). But in summer the sign of the first term in the right-hand side of (31) will change, and this term will interfere destructively with the second term of the same equation. Such interference is captured correctly by the analysis.

The diagnostic parameters of the phase smoothed analysis are the estimated frequencies and the time coefficients $\vec{s}_i$ at each stage of the seasonal cycle. Notice that in this case , a stationary part does really exists in the pattern and therefore the stationary part identified is not due to errors in the estimation as in the 'simplified' case. Consequently the entire $\vec{s}_i$ coefficients, and not only its cyclostationary parts have to be considered for the diagnostic. Fig 14 represents the time coefficients of pair of POP 1/2 identified in the benchmark field by the 'phase smoothed' method at stages corresponding to four different seasons. While the frequency of the signal can be identified in all the other seasons, coefficients in summer are mostly noise.

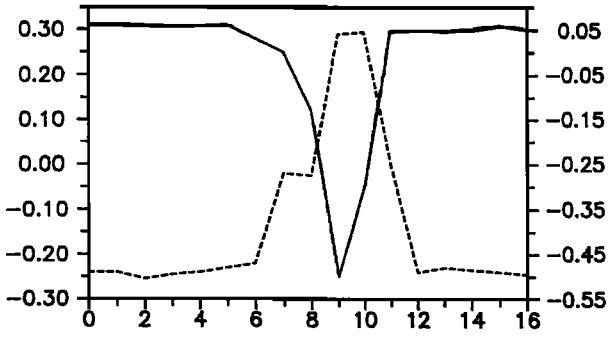

Figure 13. Benchmark field with $\theta = 0$. Results of the fixed phase analysis. Seasonal evolution of the real part of the exponents γ_1 (solid line) and γ_3 (dashed one). Units as in Figure 4.

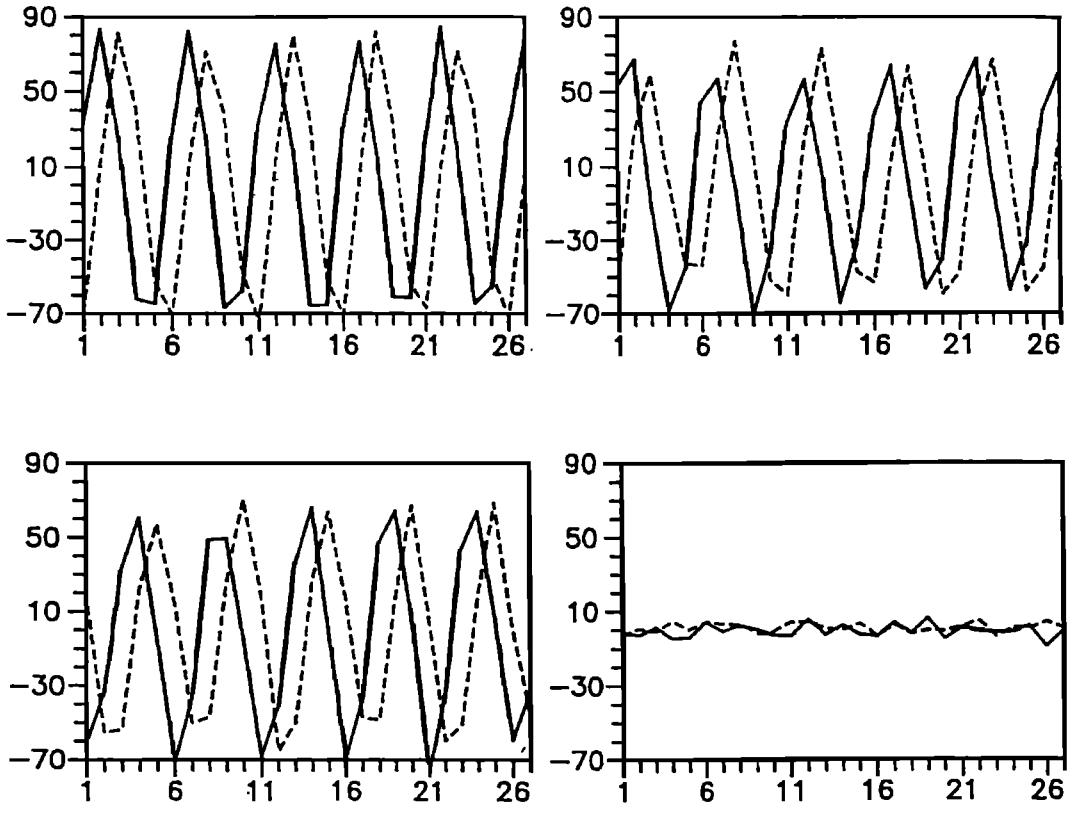

Figure 14. Benchmark field with $\theta = 0$. Results of the phase smoothed analysis. Time coefficients of the patterns 1 (solid) and 2 (dashed) sorted by the season. Units as in Figure 11.

5.3. Accuracy in the Determination of the Wave Characteristics

It has been shown by the analysis of the simplified field, that errors in the determination of the Floquet exponents can be estimated by the stationary part of the identified POP. A simple analysis suggests that in some cases a reformulation of the cyclostationary dependence of the dynamical matrix in terms of the $\tan(\omega_a t)$ and $\text{cotan}(\omega_a t)$ (ω_a being the cyclostationary frequency) instead of sine and cosine of the same argument, as was originaly proposed. Both ways were implemented and set to the analysis of the simplified version of our benchmark field. The stationary patterns (which measure the error in this case) were stronger when using the sine and cosine than when using the tangent and cotangent formulation.

In all the analyses carried out for the present work, the phase smoothed approach gave a better estimation of the POP frequency than the other method. However, the analysis of the empirical time coefficients $\vec{s}_t^c$ at the right season gave the best frequency's estimation.

6. Discussion

To include the cyclostationary dependence in a linear inverse model of a multivariate geophysical data field, two different methods were proposed [*Hasselmann and Barnett, 1981*]. The application of both methods to the analysis of real data (*Storch et al*,1993; *OrtizBeviá*, 1993) put forward a number of questions. The procedure reported here was intended as a way of solving them: synthetics data fields are build and analyzed with the two methods. These synthetic fields include two signals buried in noise. The signals correspond to two different geophysical waves, with spatial and time behavior well differentiated. To perform sucessfully, an analysis procedure has to be able to separate the signals, and to estimate accurately the spatial and temporal characteristics and also the seasonal dependence of each. Because the true characteristics of the signals present in the synthetic data are known, the output of the analysis performed using each of the models can be given an interpretation while the performance of both models are compared.

In the first approach the data are sorted according to the stage of the cycle or phase value. The value of the seasonal dependence for each of the subseries built in this way remains unchanged through the analysis. Because of the reduced length of the time series used for the identification of model's parameters, errors are expected to be important. The analysis performed here with this method shows that they are and as a consequence the different signals present in the data are not well estimated. For seasons where the signals are weak, the patterns are intermixed. In the second method, the phase is smoothed and modelled into the parameters of the finite difference equation system. The method succeeds at separating the signals' frequencies and at identifying the spatial patterns and is able to give a cyclic evolution but cannot label its stages (the phase).

For the case of the phase fixed method, the analysis shows how the errors in the estimation of the model parameters allow to identify the seasonal dependence directly from the eigenvalues of the forward seasonal matrices $\mathbf{B}^\kappa$. It also

points to the importance of visual inspection to detect an intermixing of the patterns and suggests that the use of the normalization condition of (22) can lead to confusion if the initial season is not well chosen (see the comments to Figures 13a, 13d in *Storch et al* [1993]. The phase smoothed method is greatly improved by this exercise. The empirical time coefficients sorted by the phase were identified as the useful parameter to label the cyclostationary dependence of the field. The idea of using the empirical time coefficients $\vec{s}_i^c$ as diagnostic parameter of the POP output is not new. In fact in some of the previous applications of the POP stationary method [*Xu and Storch*, 1990; *Penland and Magorian*, 1993], the coefficients $\vec{s}_i$ are used to estimate the frequency associated to the POP pattern with preference to the value given by the corresponding eigenvalue of the dynamical matrix.

The analyses also suggest that some features of the observed low-frequency climatic variability may have a simple explanation. For instance, the smallness of a geophysical signal (the ENSO signal) in spring has been the source of much speculation [*Xue et al.*, 1994]. This feature would account for the loss of predictability skill of coupled atmosphere - ocean models initialized at this season. It has been explained as the consequence of a destructive interference between the ENSO and the quasibiennial oscillation (QBO) signals [*Wang*, 1994]. Our analysis of the benchmark field shows that the interference between the stationary and the seasonally dependent part of the one (ENSO) signal would produce the same effect.

Only a few of the analyses of different simulations that were performed have been detailed here. Many other were carried out: on synthetic data obtained by changing the wave parameters, the phase of the cyclostationary dependence, and the amount of noise and/or the length of the time series. They have been omitted because their results were not different from the ones described here. Analysis of synthetic data where the stochastic white noise forcing was replaced by red noise without spatial structure was also carried out and always supported the conclusions obtained by using white noise in the simulations.

Appendix: Determination of the Characteristic Matrix and Floquet's Theorem

The determination of the characteristic matrix Ψ and of the fundamental state vectors $\vec{u}_k(t)$ is a somewhat involved procedure based on Floquet's theorem, which we review briefly here following *Magnus and Winkler* [1966]. Through out this review, any index that is repeated in a product is automatically summed on from 1 to n, that is $c_i\vec{y}_i(t) = \sum_{i=1}^{n} c_i\vec{y}_i(t)$.

If $\vec{r}(t)$ is an n-dimensional vector of the form $\vec{r}(t) = [r_1(t), r_2(t), ...r_n(t)]^\dagger$ that satisfies the n-dimensional differential equation system

$$d_t\vec{r}(t) = \mathbf{A}(t)\vec{r}(t) \tag{A1}$$

where the dynamical matrix $\mathbf{A}(t)$ is periodic of period T_a:

$$\mathbf{A}(t+T_a) = \mathbf{A}(t). \tag{A2}$$

Floquet's theorem states that the solutions to (A1) can always be written as

$$\vec{r}(t) = c_k exp(\mu_k \Delta t)\vec{u}_k; \Delta t = t - t_0, \tag{A3}$$

where the μ_k are Floquet's exponents (constant in time) and the $\vec{u}_k$ are no longer constant in time but periodic with period T_a.

Proof: If $\vec{y}_i(t)$ is a set of n solutions that satisfy

$$y_{ij}(0) = \delta_{ij}; \delta_{ii} = 1, \delta_{ij} = 0, i \neq j. \tag{A4}$$

Any other solution $\vec{r}(t)$ of (A1) can be written as a linear combination of this set. The values of $\vec{y}_i(t)$ for $t_0 < t < T_a$ collected into a matrix $\mathbf{Y(t)}$ form the fundamental matrix of the system. The value of $\mathbf{Y}(t = T_a) = \Psi$ yields the characteristic matrix of this cyclostationary system. Let $\vec{x}_i(t)$ with i=1,...,n be another set of n solutions that satisfy

$$\vec{x}_i(0) = \vec{z}_i = d_{ij}\vec{y}_j(0) \tag{A5}$$

where the $\vec{z}_i$ are the eigenvectors of the characteristic matrix Ψ associated to the eigenvalues ρ_i.

$$\Psi\vec{z}_i = \vec{z}_i\rho_{ii} \tag{A6}$$

and because (A1) is linear, the relationship given by (A5) will hold for any time t. Since $\vec{y}_i(t)$ are also solutions of A1, we can write

$$\vec{y}_i(T_a) = c'_{ik}\vec{y}_k(0) \tag{A7}$$

where $c'_{ik} = \psi_{ik}$, the elements of the matrix Ψ.

For any time $t = t + T_a$, and taking into account first (A5), then (A7), then (A6), $\vec{x}_i$ will take the form

$$\begin{aligned} \vec{x}_i(t+T_a) &= d_{ik}\vec{y}_k(t+T_a) = d_{ik}\psi_{kl}\vec{y}_l(t) \\ &= z_{ik}\psi_{kl}\vec{y}_l(t) = \vec{z}_i\rho_{il}\vec{y}_l(t) \end{aligned} \tag{A8}$$

that by use of (A5) can be reduced to

$$\vec{x}_i(t+T_a) = \rho_{ii}\vec{x}_i(t) \tag{A9}$$

where here no sum to repeated indexes is implied.

The $\rho_{ii} \equiv \rho_i$ are Floquet's multipliers, and from them Floquet's exponents are obtained as

$$\mu_i = \ln(\rho_i)/T_a. \tag{A10}$$

We can then show that the $\vec{u}_i(t)$ are periodic

$$\begin{aligned} \vec{u}_i(t+T_a) &= \vec{x}_i(t+T_a)exp(-\mu_i(t+T_a) \\ &= \vec{x}_i(t)exp(-\mu_i t) = \vec{u}_i(t) \end{aligned} \tag{A11}$$

where here again no sum to repeated indexes is implied. Now since any solution $\vec{r}(t)$ can be written as a linear combination of the $\vec{x}_i$, expression (A3) is true.

In our code CYPOP, which computes cyclostationary POP with the phase smoothed method, (A6) and (A10) are used to estimate the Floquet exponents and (A11) to obtain the periodic patterns $\vec{u}_i(t)$.

Acknowledgments. This work was started on a short visit to MPIM, Hamburg. I am indebted to R. LopezVellón for carrying out for me a number of the simulations and reprograming the original code in standard form. I acknowledge also the contribution of A. RuizdeElvira in the first stages of the development of the phase smoothed method. Many thanks are due to Cecile Penland, who read carefully a previous version and made many useful comments and also to one of the Journal of Geophysical Research reviewers. This work is part of a research conducted under contract CE90/006 from the EU and the Spanish CICYT.

References

Barnett, T.P., Interaction of the Monsoon and Pacific trade wind system at interannual time scales II. The tropical band. *Mon. Weather Rev.*, *12*, 2380-2387, 1984.

Blumenthal, M.B., Predictability of a coupled ocean atmosphere model, *J. Clim.* , *4*, 766-784, 1991.

Gallager, F., H von Storch, R. Schnur and G. Hannoschoeck, The POP manual, *DKRZ*, Hamburg, 1991.

Hasselmann, K., PIPs and POPs: The reduction of complex dynamical systems using Principal Interaction and Oscillation Patterns, *J. Geophys. Res.*, *93*, 11,015-11,021, 1988.

Hasselmann, K. and T.P. Barnett, Techniques of linear prediction for systems with periodic statistics, *J. Atmos. Sci.*, *38*, 1342-1347, 1981.

Magnus, W. and S.Winkler, *Hill's Equation*, Wiley - Intersci., New York, 1966.

Matsuno, T., Quasigeostrophic motions in the equatorial area, *J. Meteorol. Soc. Japan*, *44*, 25-43, 1966.

OrtizBeviá, M.J., Empirical analysis of ENSO, in *Mathematics, Climate and Environment*, edited by J. Lions and I. Diaz, Masson, Paris, 1993.

Penland, C., and T. Magorian, Prediction of Niño 3 sea surface temperature using linear inverse modelling, *J. Clim.*,*6* ,1067-1076, 1993.

Tarantola, A., *Inverse Problems Analysis*, Elsevier, New York, 1987.

Storch, H. v., G. Burger, R. Scnurr, and J. S. Xu, Principal Oscillation Pattern Analysis, *Max-Planck-Inst. für Meteorol. Rep.*,*113*,Hamburg, 1993.

Xu,J.S. and H. v. Storch, Principal Oscillation Patterns-prediction of the Southern Oscillation , *J. Clim.*,*3*,1316-1329, 1990.

Xue, S.E., M.A. Cane, S.E. Zebiak, and M.B. Blumenthal, On the prediction of ENSO: A study with a low order Markov model, *Tellus*,*46A*, 512-528, 1994.

Wang, X.L., The coupling of the annual cycle and ENSO over the Tropical Pacific, *J. Atmos. Sci.*, *51*, 1115-1136, 1994.

M.J.OrtizBeviá. Departamento de Física, Universidad de Alcalá, Apdo.20, 28880 Alcalá de Henares, Madrid, Spain. (e-mail:fsortiz@alcala.es)

(Received December 21, 1995; revised January 20, 1997; accepted January 21, 1997)